Revue des Composites et des Matériaux Avancés-Journal of Composite and Advanced Materials
Vol. 33, No. 5, October, 2023, pp. 311-316
Journal homepage: http://iieta.org/journals/rcma

Effect of Cu-Doping Levels on the Structural and Optical Properties of SnO_2 Thin Films Prepared by Chemical Spray Pyrolysis

Sundus Mohammad Meteab*, J. F. Mohammad

Department of Physics, Faculty of Education for Pure Science, University of Anbar, Anbar 31001, Iraq

Corresponding Author Email: sun21u3003@uoanbar.edu.iq

https://doi.org/10.18280/rcma.330505

Received: 14 August 2023
Revised: 2 October 2023
Accepted: 20 October 2023
Available online: 31 October 2023

Keywords:
SnO_2 thin films, Cu doping, XRD, optical properties, SnO_2:Cu, EDX, chemical spray pyrolysis, nanocrystalline films

ABSTRACT

In this research, chemical pyrolysis method was employed to synthesize nanocrystalline pure SnO_2 and copper-doped SnO_2 films (at different doping levels: 3%, 5%, and 7%) on glass substrates at 350°C. X-ray diffraction (XRD) results reveal the prepared films are polycrystalline with a tetragonal crystal structure and the intensity of peaks decreased with increased doping ratio of copper. Field Emission-Scanning Electron Microscope (FESEM) results confirm that the particle size decreases as Cu-doping increase. EDX images show the presence of Sn, Cu, and O in the structures of the prepared films. Optical results show acceptable transmittance at the middle of the visible region (80% for 7% Cu doping). Additionally, the optical energy gap of the pure SnO_2 was calculated to be 3.75 eV, and this energy gap increased to 3.90 eV with higher levels of Cu doping. The absorption coefficient decreased as the Cu doping concentration increased.

1. INTRODUCTION

Transparent conducting oxides (TCOs) are attractive materials due to good conductivity, high transparent with direct band gap energy of approximately (3.6 eV) [1-4]. In recent decades, undoped and doped materials or composites based on tin oxide (SnO_2) have been extensively studied for various practical applications, such as optical waveguides, phosphors, transparent Conductive oxides, gas sensors and UV emitters [5-7]. The properties of tin dioxide films were improved by adding several dopants, such as: Ni, Zn, F, Mg, Co, Mn and Cu [8-13]. Copper (Cu-transition metal) is an extrinsic n-type dopant with an atomic number of 29, and a face-centered cubic crystal structure, these features are useful in thin film technology. Additionally, Cu^{+} and Cu^{+2} have ionic radii that are bigger than Sn+4's (0.071) nm and 0.077 nm respectively [14, 15]. Variety methods were used to prepared pure and doped SnO_2 such as; laser ablation, chemical vapor deposition, sol-gel and spray pyrolysis (SP). Among these methods, spray pyrolysis s widely used to prepare SnO_2 films due to simplicity, cheaps and large area deposition [16]. In this work, the effect of dopant (Cu) on the structural and optical properties of SnO_2 films are investigated.

2. MATERIALS AND METHODS

Tin chloride ($SnCl_2.2H_2O$) as a source of Tin ions (Sn) with a molar concentration of (0.02 M) was used to synthesize pure SnO_2 thin film. Copper chloride ($CuCl_2$:$2H_2O$) with the same molarity (0.02 M) was used as a dopant source of Cu ions. The glass substrate (2.5cm×2.5cm) was carefully ultrasonically cleaned using different solvents (distilled water, ethanol, acetone) for 10 minute for each step. The spray pyrolysis parameters were maintained as follows: The deposition temperature (350°C), The spray pyrolysis parameters were maintained as follows: the vertical distance between the nozzle and glass substrate (30 cm), spray rate (5 second), and stop time (15 seconds). Then, the solution was sprayed on the heated substrate, and after the films were deposited the substrate was left to cool and then kept in a specific container. To obtain the required weight to be dissolved, it is found through the following equation [17]:

$$M = \left(\frac{W_t}{M_{wt}}\right).\left(\frac{1000}{V}\right) \tag{1}$$

where: M: concentration of molarities, W_t: weight, M_{wt}: molecular weight for the materials used, V: volume of distilled water.

3. RESULTS AND DISCUSSION

3.1 XRD analysis

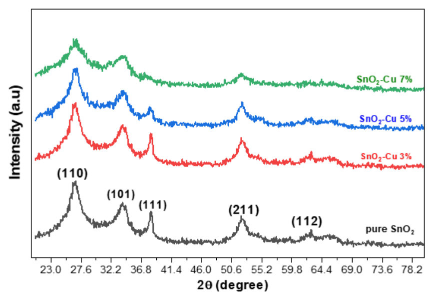

Figure 1. X-ray diffraction of pure SnO_2 film Cu:SnO_2, with Cu: (3%, 5%, and 7%)

Table 1. XRD results for pure SnO_2 and Cu:SnO_2 film

Sample	2θ (deg.)	d(hkl) (Å)	(hkl)	Crystllite Size
SnO_2 Pure	26.35	3.378	110	11.46
SnO_2:Cu 3%	26.61	3.346	110	5.25
SnO_2:Cu 5%	26.63	3.343	110	4.60
SnO_2:Cu 7%	26.68	3.337	110	4.02

X-ray diffraction was studied to know the nature of the crystal structure of different materials and the crystalline phases in which they can exist. Figure 1 shows the X-ray diffraction spectra of pure SnO_2 and Cu-doped SnO_2 (3, 5 and, 7%). The appearance of many peaks indicates that the prepared films are polycrystalline with a tetragonal structure with a preferred orientation of plane (110). The peaks appear at 2θ = 26.35°, 33.72°, 37.78°, 51.63°and 64.23° correspond to the planes (110), (101), (111), (211) and (112) respectively. This result is agreement with the standard reported (JCPDS card SnO_2, No. 41-1445). Using Debye-Scherrer's formula (Eq. (1)) [8], the crystallite size (D) of the pure and Cu-doped SnO_2 films was calculated from the preferred direction (110) and the results are summerized in Table 1.

$$D = \frac{0.9\,\lambda}{\beta\cos\theta} \tag{2}$$

where, β is the full width at half maximum (FWHM), λ is the wavelength of X-ray (0.15406 nm), and θ is the diffraction angle. As the dopant ratio increases from (3% to 7%), the intensity decreases, and FWHM increases which causes the crystalline size to decrease.

3.2 FE-SEM analysis

Figure 2 shows scanning electron microscope images of pure SnO_2 and Cu:SnO_2 films with Cu ratios of (3%, 5%, and 7%) deposited on a glass substrate by chemical spray pyrolysis method. It is noted that the pure SnO_2 films consist of a homogeneous dense distribution consisting of different shapes, where small grains gather as a result of the deposition process and create large aggregates randomly distributed on the surface. The average particle size of the pure SnO_2 is approximately (76.44 nm). As for the Cu-doped SnO_2 films with ratios of Cu: (3%, 5%, 7%), it is noted that with an increase in the doping Cu percentage, the shape and size of the particles change to become semi-spherical, where the particles are linked to each other to form aggregates of clusters, these aggregates are also associated with other large granules, which are distributed randomly on the surface of the film. With an increasing doping ratio of Cu, the particle size decreases from (38.47, 25.35, and 20.37 nm) for 3% Cu:SnO_2, 5% Cu:SnO_2, and 7% Cu:SnO_2 respectively. This result is consistent with the results of XRD and in agreement with the results of reference [18].

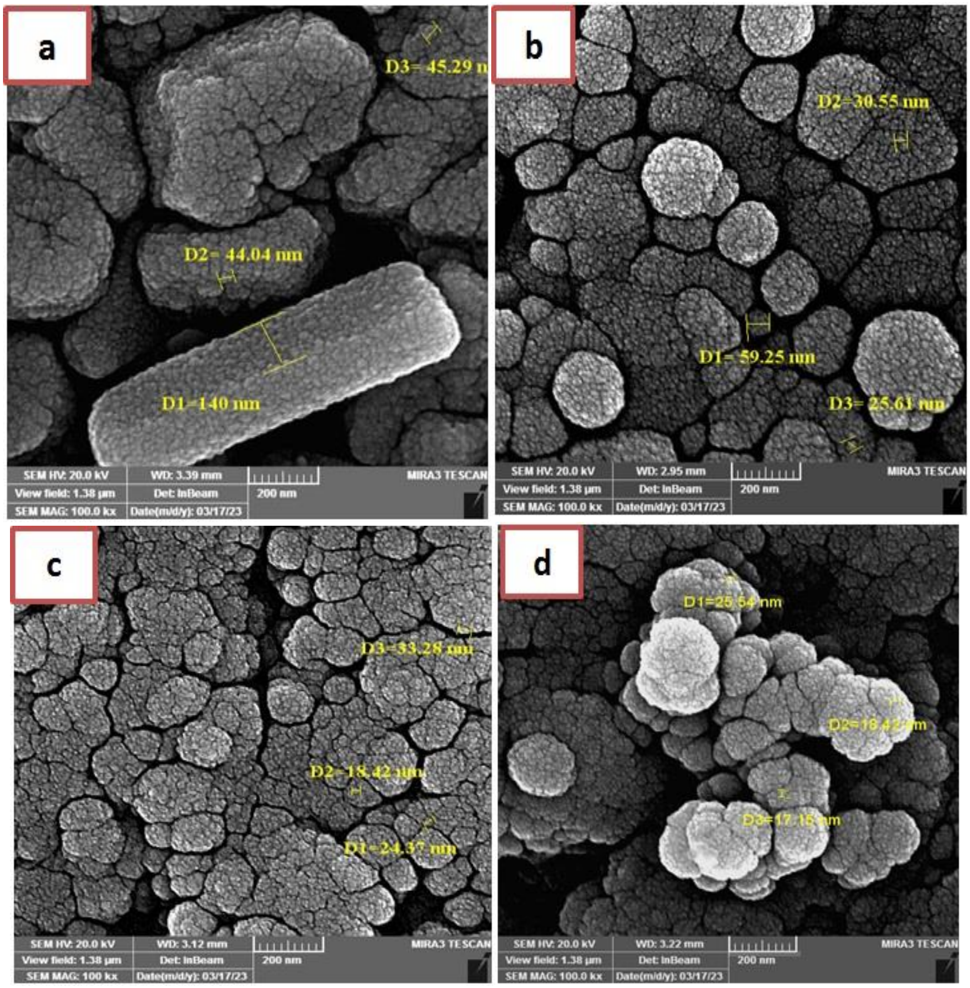

Figure 2. FE-SEM images of: (a) pure SnO_2, (b) SnO_2:3%Cu, (c) SnO_2:5%Cu, (d) SnO_2:7%Cu

3.3 EDX analysis

Figure 3 shows energy dispersive X-ray (EDX) images of pure tin oxide and copper-doped tin oxide with three different ratios of copper (3%, 5%, and 7%) and the results are as shown in Table 2. EDX analysis of the SnO_2 thin film confirms the presence of tin, and oxygen elements. The presence of Silicon (Si) is a result of the chemical glass structure, while the presence of gold (Au) element in EDX- image due to using gold plating in order to improve FE-SEM results. For the copper-doped tin oxide, we note the appearance of the previously mentioned elements in addition to the copper element. In general, increasing the doping percentage of copper in the deposition solution leads to an increase in the concentration of copper in the tin oxide film.

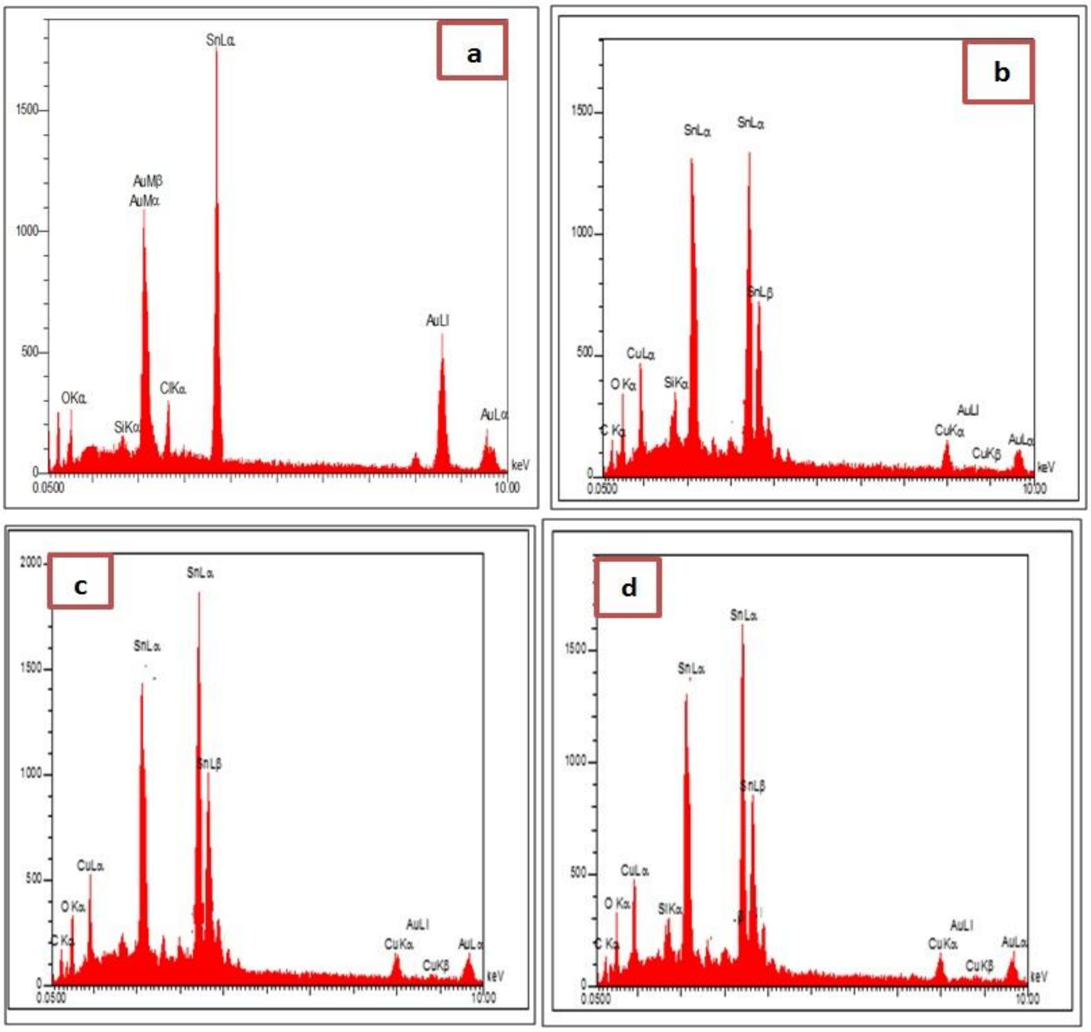

Figure 3. EDX images of: (a) pure SnO_2, (b) SnO_2:3%Cu, (c) SnO_2:5%Cu, (d) SnO_2:7%Cu

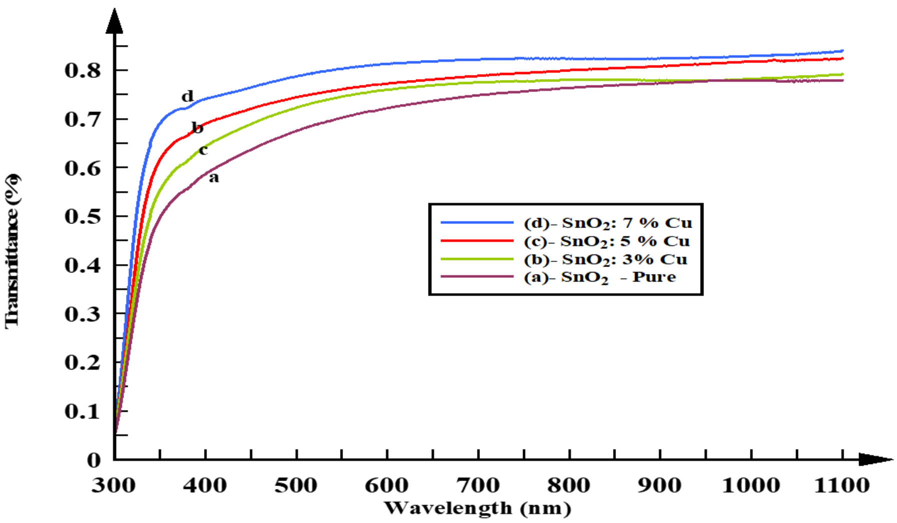

Figure 4. Optical Transmittance of: (a) pure SnO_2, (b) SnO_2:3%Cu, (c) SnO_2:5%Cu, (d) SnO_2:7%Cu

Table 2. EDX results for pure SnO_2 and Cu:SnO_2 film

Element (Wt%)	Sn	O	Cu
Pure SnO_2	91.21	8.79	----
Cu 3%	89.69	7.75	2.56
Cu 5%	92.85	4.20	2.95
Cu 7%	93.05	3.02	3.93

3.4 Optical properties analysis

Figure 4 presents the optical transmission of undoped and Cu-doped SnO_2 thin films as functions of wavelength in the range (300–1100 nm). According to Figure 4, the average transmission in the middle of the visible region is approximately (70%) and the transmittance increases with increasing the Cu dopant up to 80% for SnO_2:7%Cu. Increasing the percentage of doping, copper atoms (Cu) work to attract the largest possible number of electrons, which increases the transmittance and causes a decrease in the absorbance [19]. The transparency is related to the structural (such as crystallinity and roughness) and surface properties, so less reflectivity and better crystallinity lead to an increase in the transmittance, and this is achieved by dopant SnO_2 with Cu.

Figure 5 shows the absorption coefficient (α) as a function of wavelength for pure SnO_2 and Cu-doped SnO_2 with dopant ratios (3%, 5%, 7%). It is evident that the absorption coefficient decreases with the increased dopant ratio of copper. This result may be attributed to decreases in the film thickness to be thinner as a result of increasing the copper doping percentage, which decreases the optical path inside the prepared film. This result is in agreement with the results of reference [20].

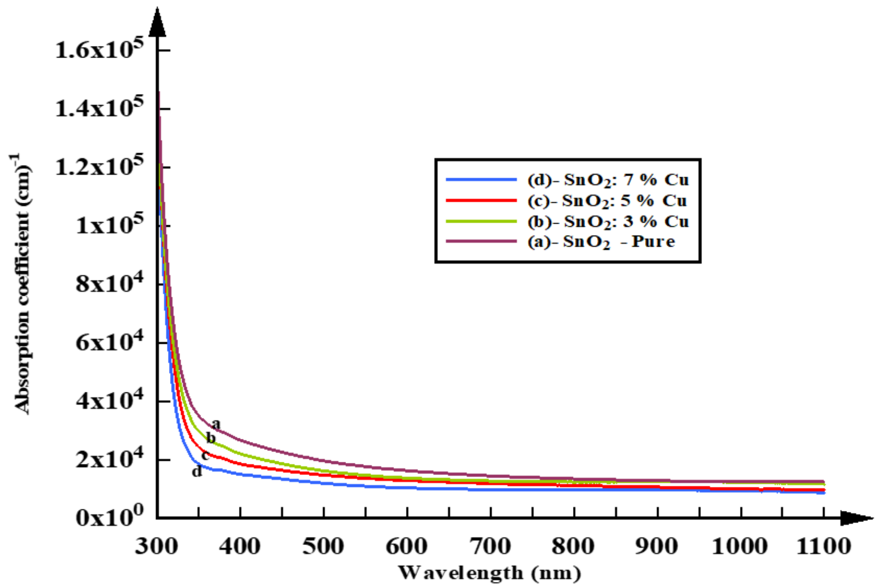

Figure 5. Absorption coefficient of: (a) pure SnO_2, (b) SnO_2:3%Cu, (c) SnO_2:5%Cu, (d) SnO_2:7%Cu

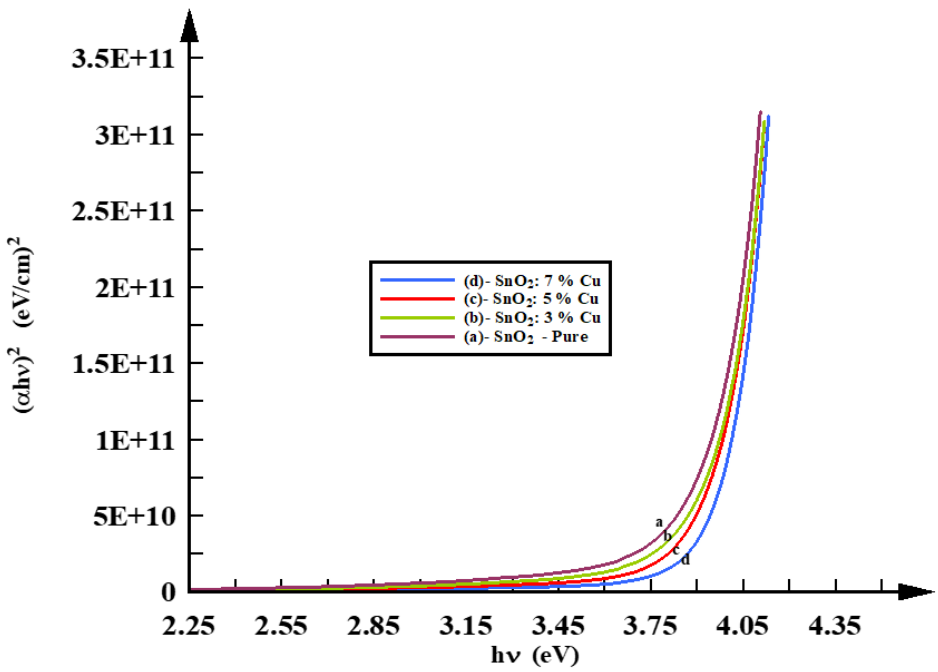

Figure 6. Energy gap of: (a) pure SnO_2, (b) SnO_2:3%Cu, (c) SnO_2:5%Cu, (d) SnO_2:7%Cu

Figure 6 shows the optical energy gap of SnO_2 that has been doped with three different ratios of Cu (3, 5, and 7%). In light of this, the (hυ) values are plotted as a function of photon energy $(\alpha h\nu)^2$ determined by the Tauc equation [21].

$$(ahv)^2 = B\left(hv - E_g\right)^{\frac{1}{2}} \quad (3)$$

As copper doping increases, the energy gap widens. The band gap of pure SnO_2 was (3.75 eV) and increased with the addition of copper doping ratio. Eg values for nanocrystalline SnO_2:Cu (3, 5, and 7%) are (3.80, 3.85, and 3.90 eV). It is noted that the optical energy gap expanded and the absorbance decreased as the dopant ratio of Cu increased, which leads to producing levels in the forbidden energy gap that are close to the conducting band. The absorption edge was moved up towards higher energies as a result [22].

4. CONCLUSIONS

The influence of Cu doping on the structural and optical properties of SnO_2 thin films has been investigated. The synthesis of SnO_2 and Cu doped SnO_2 thin films were polycrystalline with a tetragonal structure, according to XRD data. The crystallite size decreases with increased Cu ratio for all thin films. EDX results showed that tin and copper are present within the film composition. The optical transmittance of the prepared films is more than 70% and increases with increasing copper doping. The optical energy gap of the SnO_2 film increases with increasing copper doping ratio and is (3.80, 3.85, and 3.90 eV) for the copper doping ratios (3, 5, and 7%), respectively. These results suggest that the Cu-doped SnO_2 thin films have potential applications for many applications, especially as a window layer for solar cells.

REFERENCES

[1] Stadler, A. (2012). Transparent conducting oxides-an up-to-date overview. Materials, 5(4): 661-683. http://doi.org/10.3390/ma5040661

[2] González, G.B. (2012). Investigating the defect structures in transparent conducting oxides using X-ray and neutron scattering techniques. Materials, 5(5): 818-850. http://doi.org/10.3390/ma5050818

[3] Krishna, R.M., Hayes, T.C., Krementz, D., Weeks, G., Torres, A.M., Brinkman, K., Mandal, K.C. (2012). Characterization of transparent conducting oxide thin films deposited on ceramic substrates. Materials Letters, 66(1): 233-235. https://doi.org/10.1016/j.matlet.2011.08.066

[4] Lewis, B.G., Paine, D.C. (2000). Applications and processing of transparent conducting oxides. MRS Bulletin, 25(8): 22-27. https://doi.org/10.1557/mrs2000.147

[5] Warda, D., Noubeil, G., Kamel, M. (2021). A Comparative study on the optoelectronic performance of undoped, mg-doped and F/Mg Co-doped ZnO nanocrystalline thin films for solar cell applications. Journal of Nanoelectronics and Physics, 3(6): 06016. https://doi.org/10.21272/jnep.13(6).06016

[6] Guermat, N., Darenfad, W., Mirouh, K. (2021). ‘Annealing temperature effect on optoelectronic properties of ZnO/8% F/1% Co/3% Mg thin films synthesis by spray pyrolysis. Algerian Journal of Engineering Architecture and Urbanism, 5(5): 873-880.

[7] Daranfed, W., Guermat, N., Mirouh, K. (2020). Experimental study of precursor concentration the Co_3O_4 thin films used as solar absorbers. Annales de Chimie-Science des Matériaux, 44(2): 121-126. https://doi.org/10.18280/acsm.440207

[8] Khalfallah, M., Guermat, N., Daranfed, W., Bouarissa, N., Bakhti, H. (2020). Hydrophilic nickel doped porous SnO_2 thin films prepared by spray pyrolysis. Physica Scripta, 95(9): 095805. http://doi.org/10.1088/1402-4896/aba8c5

[9] Guermat, N., Darenfad, W., Mirouh, K., Bouarissa, N., Kalfallah, M., Herbadji, A. (2022). Effects of zinc doping on structural, morphological, optical and electrical properties of SnO_2 thin films. The European Physical Journal Applied Physics, 97: 14. http://doi.org/10.1051/epjap/2022210218

[10] El Jouad, M., Garmim, T., Louardi, A., Hartiti, B., Monkade, M., Touhtouh, S., Hajjaji, A. (2022). Elaboration and characterization of Ni and Al co-doped SnO_2 thin films prepared by spray pyrolysis technique for photovoltaic applications. Materials Science and Engineering: B, 286: 116044. https://doi.org/10.1016/j.mseb.2022.1160440

[11] Khelifi, C., Attaf, A., Yahia, A., Dahnoun, M. (2019). Investigation of F doped SnO_2 thin films properties deposited via ultrasonic spray technique for several applications. Surfaces and Interfaces, 15: 244-249. http://doi.org/10.1016/j.surfin.2019.04.001

[12] Skariah, B., Naduvath, J., Thomas, B. (2016). Effect of long term ageing under humid environment on the LPG sensing properties and the surface composition of Mg-doped SnO_2 thin films. Ceramics International, 42(6): 7490-7498. http://doi.org/10.1016/j.ceramint.2016.01.155

[13] Gupta, P., Rathore, V., Sahoo, S., Majumder, S. (2023). Investigation of electronic properties of Mn doped SnO_2 thin film. Vacuum, 211: 111914. https://doi.org/10.1016/j.vacuum.2023.111914

[14] Somjaijaroen, N., Sakdanuphab, R., Chanlek, N., Chirawatkul, P., Sakulkalavek, A. (2019). Simultaneous O_2 plasma and thermal treatment for improved surface conductivity of Cu-doped SnO_2 films. Vacuum, 166: 212-217. http://doi.org/10.1016/j.vacuum.2019.05.017

[15] Divya, J., Pramothkumar, A., Gnanamuthu, S.J., Victoria, D.B. (2020). Structural, optical, electrical and magnetic properties of Cu and Ni doped SnO_2 nanoparticles prepared via Co-precipitation approach. Physica B: Condensed Matter, 588: 412169. https://doi.org/10.1016/j.physb.2020.412169

[16] Chen, A., Xia, S., Ji, Z., Xi, J., Qin, H., Mao, Q. (2017). Effects of Cu doping on the structure, electronic and optical properties of SnO_2 thin films by spray pyrolysis: An experimental and density functional study. Surface and Coatings Technology, 322: 120-126. https://doi.org/10.1016/j.surfcoat.2017.05.026

[17] Neaman, D.A. (1992). Semiconductor physics and devices. Irwin.

[18] Al-Jawad, S.M., Elttayf, A.K., Saber, A.S. (2017). Studying structural, optical, electrical, and sensing properties of nanocrystalline SnO_2: Cu films prepared by sol–gel method for CO gas sensor application at low temperature. Surface Review and Letters, 24(8):

1750110. http://doi.org/10.1142/S0218625X17501104
[19] Nilavazhagan, S., Muthukumaran, S. (2015). Investigation of optical and structural properties of Fe, Cu co-doped SnO_2 nanoparticles. Superlattices and Microstructures, 83: 507-520. http://doi.org/10.1016/j.spmi.2015.03.036
[20] Kathalingam, A., Kesavan, K., Rana, A.U.H.S., Jeon, J., Kim, H.S. (2018). Analysis of Sn concentration effect on Morphological, Optical, Electrical, and photonic properties of Spray-coated Sn-doped Cdo Thin Films. Coatings, 8(5): 167. http://doi.org/10.3390/coatings8050167
[21] Tauc, J. (1974). Amorphous and Liquid Semiconductors. Springer, London, 10: 978-1. http://doi.org/10.1007/978-1-4615-8705-7
[22] Tombak, A., Ocak, Y.S., Bayansal, F. (2019). Cu/SnO_2 gas sensor fabricated by ultrasonic spray pyrolysis for effective detection of carbon monoxide. Applied Surface Science, 493: 1075-1082. http://doi.org/10.1016/j.apsusc.2019.07.087